Momentum Transfer to a Surface When Irradiated by a High-Power Laser

Girard A. Simons*
Physical Sciences Inc., Andover, Massachusetts

A simplified model is developed to predict the impulse imparted to a surface when irradiated by a high-power laser. A high-pressure plasma is created by a laser-supported detonation (LSD) wave traveling toward the energy source. The multidimensional expansion of the high-pressure region is described by patching one-, two-, and three-dimensional blast wave solutions to the LSD wave. The patching times are obtained by conserving energy between the wave solutions and are shown to be different from those used by previous authors. The pressure-time-space results are integrated to determine the net impulse delivered to the surface. A simplified procedure is outlined for converting target failure criterion to laser parameter requirements.

Introduction

WHEN a single-pulse high-power laser irradiates a target surface, a laser-supported detonation wave (LSD) forms above the target surface and propagates into the background gas. The high-pressure gas behind the LSD wave transfers momentum to the target and represents a potential damage mechanism. A measure of the efficiency with which momentum is imparted to the target is the coupling coefficient, defined as the impulse per unit laser energy. Several authors[1-4] have sought to evaluate and optimize the coupling coefficient with respect to the laser beam diameter, pulse duration, and energy.

The impulse imparted to the target during irradiation is a small fraction of the total impulse delivered. Hence, an accurate description of the momentum transfer must include the decay of the LSD wave into a hydrodynamic blast wave. The transition from an LSD wave to a blast wave has been described[1,3,4] by patching the blast wave and LSD wave solutions together at an intermediate time. Hydrocode simulations[2] have confirmed this approach but a unique choice for the patch time was not established. It is shown herein that various choices for the patch time results in variations in the energy in the blast wave. Since the energy in the blast wave must be equal to the laser energy deposited in the LSD wave, the patch time may be established by specifying the energy in the asymptotic blast wave. Using this technique to determine the patch time, it is shown that the laser energy required to deliver a fixed impulse to a target may, in some limits, be a factor of five greater than previously assessed.

Patched Solutions

The high-pressure plasma generated by the LSD wave imparts momentum to the target until a relaxation wave penetrates the plasma from the surrounding low-pressure ambient environment. The relaxation may occur from the axial (laser beam) direction in time τ_z or laterally in time τ_{2D}. The time scales τ_z and τ_{2D}, and the pressure decay laws between these time scales, control the total momentum imparted to the target by the laser. The LSD wave is patched to conventional one-, two-, and three-dimensional blast wave solutions at the times τ_z and τ_{2D}. The patching sequence varies with the relative magnitude of these time scales.

If the axial relaxation time τ_z is less than τ_{2D} (case I) the LSD wave will propagate at constant velocity and pressure until time τ_z when the wave forms a one-dimensional blast wave (1DBW). The 1DBW will propagate to time τ_{2D}, at which time it will form a three-dimensional blast wave (3DBW). These patched solutions are normalized to pressure p_s which represents the pressure of the LSD wave on the surface of the target. For case I,

$$t<\tau_z: \quad p=p_s \qquad \text{LSD} \qquad (1)$$

$$\tau_z<t<\tau_{2D}: \quad p=p_s\left(\frac{\tau_z}{t}\right)^{2/3} \qquad \text{1DBW} \qquad (2)$$

$$\tau_{2D}<t: \quad p=p_s\left(\frac{\tau_z}{\tau_{2D}}\right)^{2/3}\left(\frac{\tau_{2D}}{t}\right)^{6/5} \qquad \text{3DBW} \qquad (3)$$

Similarly, for $\tau_{2D}<\tau_z$ (case II), the LSD wave forms a two-dimensional blast wave (2DBW) at time τ_{2D} and a 3DBW at time τ_z. The solutions for the pressure in case II are

$$t<\tau_{2D}: \quad p=p_s \qquad \text{1DLSD} \qquad (4)$$

$$\tau_{2D}<t<\tau_z: \quad p=p_s\left(\frac{\tau_{2D}}{t}\right) \qquad \text{2DBW} \qquad (5)$$

$$\tau_z<t: \quad p=p_s\left(\frac{\tau_{2D}}{\tau_z}\right)\left(\frac{\tau_z}{t}\right)^{6/5} \qquad \text{3DBW} \qquad (6)$$

The critical element in utilizing the patched solution is that of specifying τ_z and τ_{2D}. Pirri[1] required that axial relaxation occurred when the laser pulse terminated, i.e., τ_z equals the duration of the laser pulse, τ_p. Ferriter et al.[2] argued that axial relaxation could not occur until an acoustic wave traveled from the LSD wave to the target surface, notifying the target that the laser pulse was off. Neglecting the finite velocity of the gas behind the LSD wave, Ferriter obtained $\tau_z=2.83\tau_p$, whereas τ_z is shown to be $3.23\tau_p$ when the finite velocity of the gas is included.[4] Similar arguments have been utilized to evaluate τ_{2D}. Since the velocity of sound behind an LSD wave is of the order of the velocity of the wave, V_w, τ_{2D} is of the order of R_s/V_w where R_s is the radius of the irradiated spot.

Received Oct. 24, 1983.

*Principal Research Scientist. Member AIAA.

The above choices for τ_z and τ_{2D} do not insure that the asymptotic description of the blast wave is valid. The blast wave solution for the pressure may be expressed as $p(E,t)$ where E is the deposition energy. Various choices for τ_z and τ_{2D} in Eqs. (2), (3), (5), and (6) will inadvertently alter the energy in the blast wave. This suggests that there must be appropriate values of τ_z and τ_{2D} that constrain the energy in the blast wave to be equal to that deposited by the LSD wave. Subsequently, the values of the patch times are determined via this criterion. In some cases, the patch times and blast wave solutions are distinctly different from those discussed previously.

Asymptotic Evaluation of the Patching Times

The variables in the patched pressure solutions [Eqs. (1-6)] are determined directly from the LSD and blast wave solutions. The LSD wave is expressed in terms of the laser intensity I_0, gas density ρ, and the ratio of specific heats γ. The velocity V_w and pressure p_w of the LSD wave,[5] and the pressure p_s on the target[1] are

$$V_w = a_1 (I_0/\rho)^{1/3}, \qquad p_w = a_2 (I_0^2 \rho)^{1/3}, \qquad p_s = a_3 (I_0^2 \rho)^{1/3}$$

respectively, where

$$a_1 = [2(\gamma^2 - 1)]^{1/3}, \qquad a_2 = a_1^2/(\gamma + 1)$$

$$a_3 = [(\gamma + 1)/2\gamma]^{2\gamma/(\gamma-1)} a_2$$

The time scale τ_z may be obtained from Eq. (2) and the known[6] 1DBW solution for the pressure at the point of the energy deposition

$$p \doteqdot 0.11 \rho (E_1/\rho t)^{2/3}$$

where the constant has been evaluated for $\gamma = 1.2$ and E_1 is the energy per unit area deposited by the laser

$$E_1 = I_0 \tau_p$$

The above expression for $p(E_1,t)$ at the target surface is identical to that given by Eq. (2) if, and only if,

$$\tau_z = \alpha \tau_p \qquad \text{(case I)} \tag{7}$$

where $\alpha \doteqdot 0.6$ for $\gamma = 1.2$.

Note that the axial relaxation time is less than the laser pulse duration. This is clearly incorrect when viewed locally at time τ_p. However, the dominant momentum transfer occurs during the asymptotic portion of the blast wave and the local details are sacrificed in order to predict the asymptotic behavior accurately.

When the lateral relaxation time is short compared to the axial relaxation time, a cylindrical blast wave forms above the target surface while the LSD wave continues to move toward the laser. The energy deposited per unit length perpendicular to the target surface is

$$E_2 = I_0 \pi R_s^2 / V_w$$

and the asymptotic blast wave solution is[6]

$$p \doteqdot 0.05 \rho (E_2/\rho)^{1/2} (1/t)$$

for $\gamma = 1.2$. Comparing this expression for $p(E_2,t)$ to Eq. (5), τ_{2D} becomes

$$\tau_{2D} \doteqdot \alpha R_s / V_w \qquad \text{(case II)} \tag{8}$$

which is again slightly shorter than one would assess from a local analysis.

The axial relaxation time τ_z as given by Eq. (7) is valid only for $\tau_z < \tau_{2D}$, whereas the lateral relaxation time τ_{2D} as given by Eq. (8) is valid only for $\tau_{2D} < \tau_z$. In both cases, the expansion fan propagates through the hot, high-density gas with a velocity approximately equal to V_w. The length scales corresponding to τ_z and τ_{2D} are $V_w \tau_p$ and R_s, respectively. Hence, the relaxation times are approximately τ_p and R_s/V_w, respectively.

If the lateral relaxation occurs first, the axial relaxation τ_z must be greater than given by Eq. (7) because the axial expansion is now occurring in a colder, lower density gas. Similarly, if the axial relaxation occurs first, the lateral relaxation time τ_{2D} must be greater than given by Eq. (8) because now the lateral expansion is occurring in a colder, lower density gas. To evaluate these limits, both Eqs. (3) and (6) are required to be identical to the asymptotic 3DBW solution. This requirement yields

$$\tau_{2D} = \alpha [R_s^3/\tau_p V_w^3]^{1/2} \qquad \text{(case I)} \tag{9}$$

and

$$\tau_z = \alpha V_w \tau_p^2 / R_s \qquad \text{(case II)} \tag{10}$$

Equations (7-10) represent a complete set of time scales for the patched pressure solutions [Eqs. (1-6)] and clearly define the range of validity of case I and case II in terms of the known variables τ_p, R_s, and V_w.

Case I $(\tau_z < \tau_{2D})$: $\tau_p < R_s/V_w$

Case II $(\tau_{2D} < \tau_z)$: $R_s/V_w < \tau_p$

The solution for the total momentum imparted to a target surface may be generated through spatial and temporal integrations of the patched pressure solutions. To accomplish this, patched solutions for the spatial extent of the blast wave must be developed first.

Patched Solutions for the Spatial Extent of the Blast Waves

The expressions for the lateral extent of the high-pressure zone are obtained by again patching blast wave solutions. For $\tau_z < \tau_{2D}$ (case I), the lateral coordinate R is equal to the spot radius R_s during the LSD wave and the 1DBW, followed by the 3DBW solution for $t > \tau_{2D}$. This is expressed as

$$t < \tau_{2D}: \qquad R = R_s \qquad \text{LSD, 1DBW} \tag{11}$$

and

$$\tau_{2D} < t: \qquad R = m_1 R_s \left(\frac{t}{\tau_{2D}}\right)^{2/5} \qquad \text{3DBW} \tag{12}$$

where m_1 is a constant of order unity. Equation (12) is identical to the 3DBW solution if, and only if, $m_1 \doteqdot 1.0$.

Similarly, for case II $(\tau_{2D} < \tau_z)$, the lateral extent of the high-pressure zone is given by

$$t < \tau_{2D}: \qquad R = R_s \qquad \text{LSD} \tag{13}$$

$$\tau_{2D} < t < \tau_z: \qquad R = m_2 R_s (t/\tau_{2D})^{1/2} \qquad \text{2DBW} \tag{14}$$

$$\tau_z < t: \qquad R = m_3 R_s (\tau_z/\tau_{2D})^{1/2} (t/\tau_z)^{2/5} \qquad \text{3DBW} \tag{15}$$

Matching the above blast wave solution to the conventional solutions[6] yields

$$m_2 \doteqdot 1.0 \quad \text{and} \quad m_3 \doteqdot 1.0$$

The 2DBW solution appropriate to case II is valid if, and only if, the two-dimensional shock radius R is less than or equal to the target radius R_t. Beyond R_t, the blast wave becomes three-dimensional, independent of τ_z! Defining τ_e as the time at which $R=R_t$, Eq. (14) yields

$$\tau_e=\alpha R_t^2/R_s V_w \tag{16}$$

and the case II solutions are valid only if $\tau_z<\tau_e$. In this limit, the blast wave undergoes transition from 2D to 3D before it reaches the edge of the target.

Whenever $\tau_e<\tau_z$, the blast wave undergoes transition from 2D to 3D at the edge of the target, prior to time τ_z. In this limit, modifications to the case II solutions are necessary. The 3DBW solution must be continuous with Eqs. (5) and (14) at $R=R_t$. The 3D solutions become

$$p=p_s(\tau_{2D}/\tau_e)(\tau_e/t)^{6/5} \qquad \text{3DBW} \tag{17}$$

and

$$R=R_s(\tau_e/\tau_{2D})^{1/2}(t/\tau_e)^{2/5} \qquad \text{3DBW} \tag{18}$$

respectively. This solution does not allow the laser and blast wave energies to be identical. Laser energy is still being deposited by the LSD wave when the cylindrical blast wave reaches the edge of the target. Only that portion of the laser energy deposited in time τ_e is contained in the 3DBW.

The above limit suggests that case II can be restricted to $\tau_{2D}<\tau_z<\tau_e$ and case III can be defined to describe the limit of $\tau_e<\tau_z$. Expressions for τ_z and τ_{2D} appropriate to case III are identical to those in case II. The case III solutions for $p(t)$ and $R(t)$ are the case II solutions, with Eqs. (17) and (18) replacing Eqs. (6) and (15), respectively. The time at which the 2DBW solution transforms into a 3DBW is now τ_e rather than τ_z. The case I, II, and III solutions are illustrated in Figs. 1-3, respectively, and have been expressed in a form that will be used to determine the net momentum transferred to the target.

Momentum Imparted to the Target

The total impulse I imparted to the target is the spatial and temporal integral of the pressure times the area.

$$I=\int_{\text{all } t}\int_0^R p(t)2\pi r\,dr\,dt \tag{19}$$

The patched solutions for $p(t)$ and $R(t)$ are illustrated in Figs. 1-3 for laser pulses of increasing time duration. The case I solutions, appropriate for short laser pulses, are illustrated in Fig. 1 and depict an LSD wave transforming into a 1DBW at τ_z and then into a 3DBW at τ_{2D}. For intermediate pulses (Fig. 2), the LSD wave transforms into a 2DBW and then into a 3DBW before reaching the edge of the target. The long pulse solution (Fig. 3) is identical to the intermediate pulse, except the 2DBW reaches the edge of the target before decaying into a 3DBW. Spatial integration of the pressure over the target surface must be terminated at either the laser spot radius R_s, blast wave radius R, or the target radius R_t, whichever is appropriate at time t. Time integrations must be terminated at the value of time for which $p(t)$ decreases to the ambient value, p_∞. There are eight distinct subcases corresponding to different values of the ambient pressure in each of the three cases. They are

Case Ia: $p\to p_\infty$ in 1DBW

Case Ib: $p\to p_\infty$ in 3DBW with $R<R_t$

Case Ic: $p\to p_\infty$ in 3DBW with $R>R_t$

Case IIa: $p\to p_\infty$ in 2DBW

Case IIb: $p\to p_\infty$ in 3DBW with $R<R_t$

Case IIc: $p\to p_\infty$ in 3DBW with $R>R_t$

Case IIIa: $p\to p_\infty$ in 2DBW

Case IIIb: $p\to p_\infty$ in 3DBW

Each subcase corresponds to different values of the laser and target parameters. The laser parameters specify the target surface pressure p_s, wave velocity V_w, pulse duration τ_p, and spot size R_s. The regions of parameter space corresponding to each subcase are illustrated in Fig. 4. Before elaborating on the solutions corresponding to each of the eight subcases, it is appropriate to discuss the approximations made in the spatial and temporal integrations of Eq. (19).

The pressure immediately behind the blast wave, p_w, is generally a factor of three greater than that at the target surface, p_s. Since the pressure decays quite rapidly behind the blast wave, the high-pressure region of the pulse is not included in the spatial integration of Eq. (19). This ap-

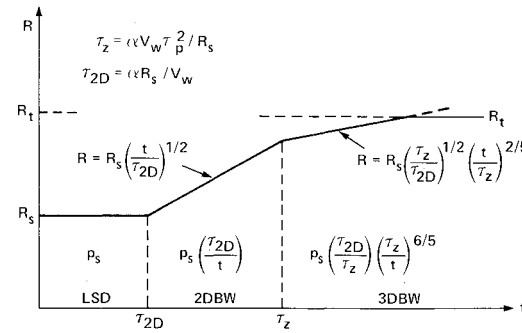

Fig. 2 Solutions for intermediate laser pulses ($R_s/V_w<\tau_p<R_t/V_w$, case II).

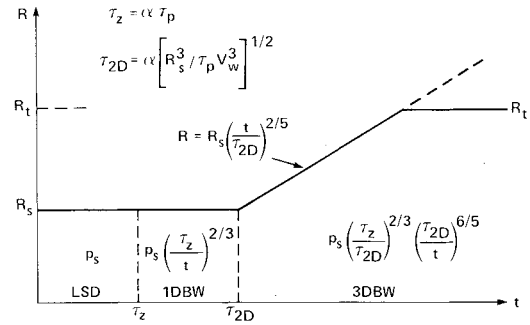

Fig. 1 Solutions for short laser pulses ($\tau_p<R_s/V_w$, case I).

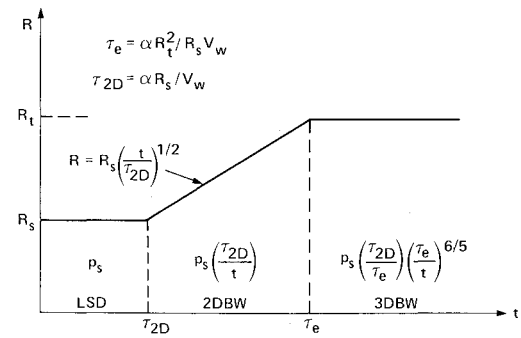

Fig. 3 Solutions for long laser pulses ($\tau_p>R_t/V_w$, case III).

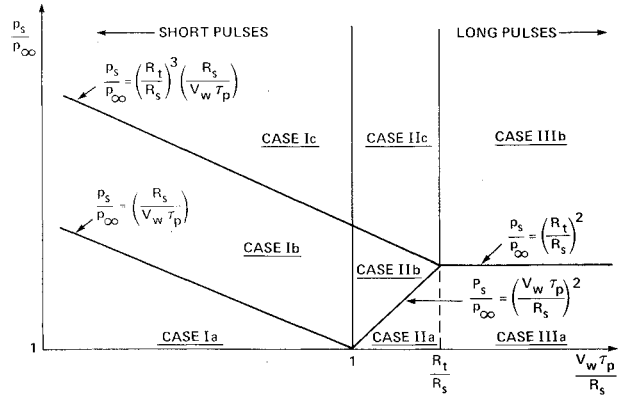

Fig. 4 Range of parameter space appropriate to each solution.

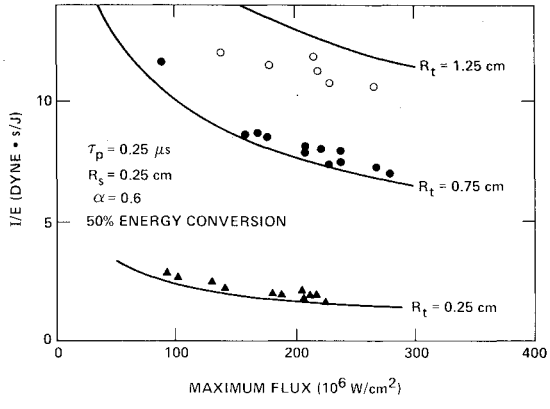

Fig. 5 Comparison of predicted impulse to data[7] for $\alpha = 0.6$.

proximation is extremely accurate when the blast wave expands beyond the target and only the uniform pressure p_s is applied to the target. However, the impulse can be underestimated by "order one" if the blast wave does not expand beyond the target [cases Ib, IIa, IIb, and IIIa].

The temporal integration of Eq. (19) is terminated when the pressure on the target surface decays to the ambient value. However, the blast wave solution is valid only for strong shocks ($p_s \gg p_\infty$) and underestimates the pressure as $p_s \to p_\infty$. This results in an underestimate of the impulse which is appreciable ("order one") only if the integral of $prdr$ is dominated by the limit at p_∞. This occurs only when the blast wave does not expand beyond the target surface as in the cases cited above.

The impulse calculations should also include the negating effect of the ambient pressure opposing that of p_s on the opposite side of the target.[4] This is appreciable (again, "order one") when the integral of $prdr$ is dominated by the limit at p_∞, i.e., for the same cases as cited above. While this tends to cancel the two effects considered above, one should expect as much as 50% errors for these cases.

Recognizing the approximations involved, the eight solutions for the total impulse imparted to the target are given below. It is straightforward to calculate p_s/p_∞, R_t/R_s, $V_w\tau_p/R_s$ and utilize Fig. 4 to determine which of the following solutions is appropriate.

Defining

$$\zeta = I/p_s \pi R_s^2 \tau_p \alpha \tag{20}$$

and

$$\zeta^* = 5\left(\frac{R_t}{R_s}\right)^{3/2}\left(\frac{R_s}{V_w\tau_p}\right)^{1/2}\left[\frac{4}{3} - \left(\frac{(R_t/R_s)^3 (R_s/V_w\tau_p)}{p_s/p_\infty}\right)^{1/6}\right] \tag{21}$$

the solutions are

Case Ia: $$\zeta = 3\left(\frac{p_s}{p_\infty}\right)^{1/2} - 2 \tag{22}$$

Case Ib: $$\zeta = \frac{5}{3}\left(\frac{p_s}{p_\infty}\right)^{1/2} + \frac{4}{3}\left(\frac{R_s}{V_w\tau_p}\right)^{1/2} - 2 \tag{23}$$

Case Ic: $$\zeta = \zeta^* + \frac{4}{3}\left(\frac{R_s}{V_w\tau_p}\right)^{1/2} - 2 \tag{24}$$

Case IIa: $$\zeta = \left(\frac{p_s}{p_\infty}\right)\left(\frac{R_s}{V_w\tau_p}\right) \tag{25}$$

Case IIb: $$\zeta = \frac{5}{3}\left(\frac{p_s}{p_\infty}\right)^{1/2} - \frac{2}{3}\left(\frac{V_w\tau_p}{R_s}\right) \tag{26}$$

Case IIc: $$\zeta = \zeta^* - \frac{2}{3}\left(\frac{V_w\tau_p}{R_s}\right) \tag{27}$$

Case IIIa: Same as IIa

Case IIIb: $$\zeta = 5\left(\frac{R_s}{V_w\tau_p}\right)\left(\frac{R_t}{R_s}\right)^2\left[\frac{6}{5} - \left(\frac{(R_t/R_s)^2}{p_s/p_\infty}\right)^{1/6}\right] \tag{28}$$

The various solutions tabulated above illustrate that there is a variety of functional relationships between impulse, pulse duration, wave velocity, spot radius, and target radius. Although the solution in each regime is relatively simple, the boundaries between the regimes are also variable and it is impossible to determine a general scaling law. A simple computer program has been written which utilizes Fig. 4 to determine the appropriate case and then calculates impulse using the corresponding analytic solution. Results are illustrated in Fig. 5 and are compared to the data of Kozlova et al.[7] The theoretical predictions agree with data if one assumes that 50% of the laser energy is absorbed by the gas. The particular point to emphasize here is the confirmation of the value of 0.6 for the constant α. Impulse scales as $1/\alpha$ for all cases. Local theories[2,4] predict that the value of α is of the order of three and the corresponding impulse predictions (via this model) are a factor of five higher. This would be consistent with the data if, and only if, the energy conversion efficiency were reduced to 10%.

The reader should be cautioned against concluding that the predictions of Ref. 4 are always a factor of five higher than those obtained here. There are several differences between the spatial and temporal solutions of the two models and there is only one limit (case Ia with $R_s = R_t$) in which this factor of five is completely apparent.

Target Damage Optimization

The analytic solutions for the impulse imparted by a high-energy laser make it relatively easy to study the effects of parametric variation. Consider the laser energy E_0, pulse duration τ_p, and spot radius R_s as the independent laser parameters. The beam intensity I_0 is expressed as

$$I_0 = E_0/\pi R_s^2 \tau_p$$

and the wave velocity and target surface pressure become

$$V_w = a_1 (E_0/\pi R_s^2 \tau_p \rho)^{1/3}$$

and

$$p_s = a_3 \rho^{1/3} (E_0/\pi R_s^2 \tau_p)^{2/3}$$

respectively. The total impulse can, for every case, be expressed as

$$I = I(E_0, \tau_p, R_t, R_s/R_t) \tag{29}$$

Ferriter et al.[2] noted that maximum impulse is delivered when the laser beam diameter matches the size of the target ($R_s = R_t$). Expressing the total impulse imparted to a particular target R_t in the form of Eq. (29), it can be shown that all expressions for I [Eqs. (22-28)] approach a maximum as $R_s \to R_t$. However, the regimes in which these solutions are valid also vary with R_s/R_t and this variation is not considered in the comparison. The results of the complete model are illustrated in Fig. 6 for a 10^4 J laser irradiating a 10 cm target. These calculations clearly demonstrate that maximum impulse is imparted when the target is flood loaded ($R_s = R_t$). Such a conclusion is, of course, subject to the constraint that R_s is not so large as to reduce the beam intensity below the LSD threshold, nor is R_s so small that the plasma is overdense.

In the limit of $R_s = R_t$, Fig. 4 reduces to three regions corresponding to cases Ia, Ic, and IIIb. The expressions for the impulse per unit area under the spot are obtained by rewriting Eqs. (22), (24), and (28), retaining only the leading term:

$$\text{Case Ia:} \quad I/A = 3\alpha p_s \tau_p (p_s/p_\infty)^{1/2}$$

$$\text{Case Ic:} \quad I/A = 8\alpha p_s \tau_p (R_s/V_w \tau_p)^{1/2}$$

$$\text{Case IIIb:} \quad I/A = 6\alpha p_s R_s / V_w$$

Structural failure of a target requires that the imparted impulse I/A exceeds some minimum value corresponding to some minimum pressure p_s. A typical failure curve is illustrated in Fig. 7. All combinations of p_s and I/A in excess of the critical level (curve ABCD) will insure failure. Since I/A and p_s are known functions of (E_0, τ_p, R_s), it is relatively straightforward to invert the solutions to determine the E_0 and τ_p required to yield a specific combination of I/A and p_s on spot radius R_s. The inversions yield

$$\text{Case Ia:} \quad E_0 = \frac{\pi R_s^2 (I/A)}{3\alpha a_3} \left(\frac{p_\infty}{\rho a_3}\right)^{1/2} \tag{30}$$

$$\tau_p = \frac{(p_\infty)^{1/2} (I/A)}{3\alpha p_s^{3/2}} \tag{31}$$

$$\text{Case Ic:} \quad E_0 = \frac{\pi R_s a_1 (I/A)^2}{64\alpha^2 \rho a_3^2} \tag{32}$$

$$\tau_p = \frac{a_1 (I/A)^2}{64\alpha^2 p_s^{3/2} R_s (\rho a_3)^{1/2}} \tag{33}$$

$$\text{Case IIIb:} \quad \frac{E_0}{\tau_p} = \frac{\pi R_s^2 p_s^{3/2}}{a_3 (\rho a_3)^{1/2}} \tag{34}$$

on

$$\frac{I}{A} = \frac{6\alpha R_s (\rho a_3 p_s)^{1/2}}{a_1} \tag{35}$$

Cases Ia and Ic correspond to regions in (I/A, p_s) space separated by

$$\frac{I}{A} = \frac{64\alpha R_s (p_\infty \rho a_3)^{1/2}}{3a_1} \tag{36}$$

whereas case IIIb reduces to a single curve in (I/A, p_s) space corresponding to particular values of E_0/τ_p. The regions are illustrated in Fig. 7. Parameter space (p_s, I/A) is separated into the three regions by direct application of Eqs. (35) and (36). That portion of the failure curve denoted by AB corresponds to case Ia. This portion of the failure curve may be transformed into (E_0, τ_p) space via Eqs. (30) and (31). Similarly, curve BC corresponds to case Ic and may be transformed into (E_0, τ_p) space via Eqs. (32) and (33). The single point on the failure curve denoted by C corresponds to a particular value of E_0/τ_p [Eq. (34)] and completes transformation of the failure curve into (E_0, τ_p) space. (Note that there is no binary combinations of laser energy and pulse duration that can achieve the conditions on curve CD.)

A relatively simple computational procedure [Eqs. (30-36)] has been outlined to transform the failure curve (p_s vs I/A) for an arbitrary target into the corresponding laser requirements (E_0 vs τ_p). An illustration of this procedure is presented in Fig. 8. The required laser energy always increases with increasing pulse duration. This is a consequence of the fact that the imparted impulse always decreases with increasing pulse duration. The laser failure criterion has three

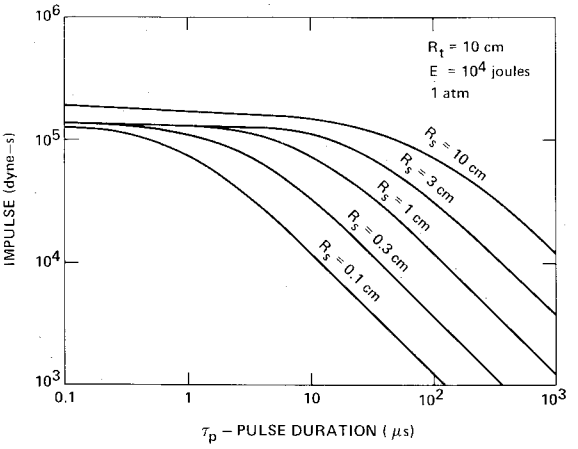

Fig. 6 Impulse imparted by a 10^4 J laser on 10 cm target.

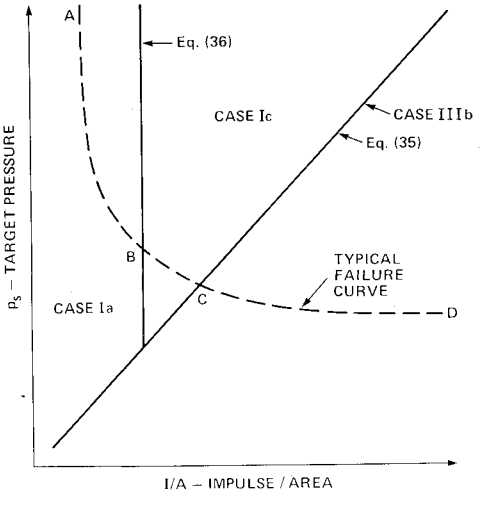

Fig. 7 Target failure criterion ($R_s = R_t$).

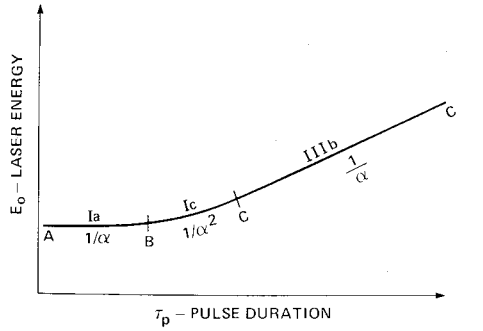

Fig. 8 Laser failure criterion ($R_s = R_t$).

distinct segments corresponding to the three possible cases. (Note that case Ia need not exist if the minimum value of I/A for target failure lies in the case Ic region.) The scaling of the laser energy with the constant α varies in each region. The energy scaling law for case IIIb is a function of the shape of the target failure curve. The energy scales as $1/\alpha$ and $1/\alpha^2$ in cases Ia and Ic, respectively. The asymptotically derived value of α ($\alpha=0.6$) is a factor of five smaller than that determined from local analysis ($\alpha \doteqdot 3$). Hence, the laser energy required to induce structural failure of the target may be five or more times greater than that which would be determined using other models. Although the asymptotic value of $\alpha=0.6$ was confirmed above with momentum transfer data,[7] its implications with respect to the required laser energy have not been confirmed.

Conclusions

An existing technique[1-4] of patching blast wave solutions together to describe the pressure field above a laser irradiated target has been modified. The impulse imparted to the target and the laser energy required to impart that impulse is a strong function of the patching times. Local analyses do not determine these times uniquely. In the present work, the conservation of energy is used to determine the patching times in a more rigorous and self-consistent manner (the value of α varies 20% depending upon which property of the blast wave is matched). Results suggest lower impulse per unit energy than previously suggested. The solutions for impulse have been reduced to simple analytic expressions which readily invert target failure criterion (pressure-impulse) into laser requirements (energy, pulse duration, spot size) for target failure.

Acknowledgments

The work reported herein was supported by the U. S. Department of Defense, Defense Nuclear Agency, and monitored by the U. S. Naval Research Laboratory under Contract N00014-81-C-2394.

References

[1] Pirri, A. N., "Theory for Momentum Transfer to a Surface with a High Power Laser," *The Physics of Fluids*, Vol. 16, Sept. 1973, pp. 1435-1440.

[2] Ferriter, N., Maiden, D. E., Winslow, A. M., and Fleck, J. A. Jr., "Laser Beam Optimization for Momentum Transfer by Laser on Supported Detonation Waves," *AIAA Journal*, Vol. 15, Nov. 1977, pp. 1597-1603.

[3] Pirri, A. N., Root, R. G., and Wu, P. K. S., "Plasma Energy Transfer to Metal Surfaces Irradiated by Pulsed Lasers," *AIAA Journal*, Vol. 16, Dec. 1978, pp. 1296-1304.

[4] Reilly, J. P., Ballantyne, A., and Woodroffe, J. A., "Modeling of Momentum Transfer to a Surface by Laser Supported Absorption Waves," *AIAA Journal*, Vol. 17, Oct. 1979, pp. 1098-1105.

[5] Raizer, Yu P., "Heating of a Gas by a Powerful Light Pulse," *Soviet Physics JETP*, Vol. 21, Nov. 1965, pp. 1009-1017.

[6] Sedov, L. I., *Similarity and Dimensional Methods in Mechanics*, edited by M. Holt, Academic Press, New York, 1959.

[7] Kozlova, N. N., Petrukhin, A. I., Pleshanov, Yu. E., Rybakov, V. A., and Sulyaev, V. A., "Measurement of Recoil Momentum for a Laser Beam Interacting with an Absorbing Surface in Air," translated from *Fizika Goreniya i Vzryva*, Vol. 11, Plenum Publishing Corp., New York, 1975, p. 650.